On the interpretation of valence bond wavefunctions

Remco W. A. Havenith,*[a] Joop H. van Lenthe,[a] Leonardus W. Jenneskens[b] and Jeroen J. Engelberts[a]

Received 3rd April 2006, Accepted 16th May 2006
First published as an Advance Article on the web 14th September 2006
DOI: 10.1039/b604721a

Valence bond wavefunctions are naturally geared to the chemist's idea of chemical bonding. In a structure one may distinguish different electron pair bonds and possible radical character. A structure may correspond to a covalent bond, where all electrons are equally divided over the atoms, or may describe an excess charge on a discrete part of the molecule, which indicates ionic bond character. From the weights of the structure in a variationally optimised multi-structure valence bond wavefunction one may derive the importance of the different bonding types. The individual structures could be considered to represent the different physical situations. We explore this concept for simple diatomic molecules and for polyatomics, and we discuss the relation to Lewis structures. We show that the assumption of individual properties for the individual structures leads to inconsistencies.

1. Introduction

The nature of the chemical bond lies at the heart of chemistry, and has as such been, and still is, a matter of interest.[1–5] Chemical bonds are classified as covalent (polar and apolar), ionic, and metallic, however, the borders between the different categories are not clear. The type of bonding on the sliding scale from apolar *via* polar to ionic, depends on the electronegativity of the atoms involved, or, to put it in other words, in the amount of electron transfer from one atom to the other. In a pure apolar, covalent bond, electrons are equally shared by the atoms, and no net electron transfer takes place. If the bond is ionic, electron transfer from one atom (polyatom fragment) to the other occurs, and the molecule is held solely together by the Coulomb attraction between them. In between these two extremes lies the polar, covalent bond, which is an admixture of the apolar and ionic bond types: electrons are shared between the two atoms forming the bond, but they are closer to the atom with the highest electronegativity.

Theoretically, bonding between two atoms can be studied by decomposition of the bond in covalent and ionic terms. However, this cannot unequivocally be performed in a molecular orbital description. Following the concept of *atoms* forming a bond by overlap of *localised* atomic orbitals, *viz*. the valence bond (VB) model, a natural decomposition occurs in ionic and covalent contributions, as both contributions are

[a] *Theoretical Chemistry Group (Affiliated to Organic Chemistry and Catalysis), Utrecht University, Padualaan 8, 3584 CH Utrecht, The Netherlands. E-mail: r.w.a.havenith@chem.uu.nl; Fax: +31-30-2537504; Tel: +31-30-2532729*
[b] *Organic Chemistry and Catalysis, Utrecht University, Padualaan 8, 3584 CH Utrecht, The Netherlands*

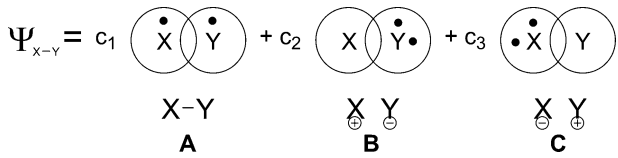

Chart 1 The valence bond wavefunction (Ψ) written as a superposition of a covalent structure **A** and the two possible ionic structures **B** and **C**. The coefficients c_i are variationally optimised in a VB calculation.

explicitly included in the wavefunction.[6] For example, for a X–Y diatomic molecule, the valence bond wavefunction is written as the superposition of a structure (**A**) corresponding to a covalent bond, and two structures (**B** and **C**) denoting the ionic component of the bond (Chart 1). If only the covalent structure **A** contributes ($c_2 = c_3 = 0$, Chart 1), the bond is purely covalent, whereas if only one of the ionic structures **B** or **C** contributes, ($c_2 = 1$ or $c_3 = 1$, Chart 1), the bond is purely ionic. In the case that c_2 and c_3 are non-zero, and unequal, the bond can be assigned to be a polar, covalent bond. From the coefficients c_i weights can be derived involving the overlap of the structures.[7]

In real (diatomic) molecules, all three structures contribute to the description of the chemical bond. In the case of delocalised bonds, *e.g.* the π-system of benzene, even more resonance structures are necessary to obtain a proper description of the bond. This analysis in terms of contributing structures relies on the equivalence of valence bond structures with Lewis structures. In this paper, this assumed equivalence and the meaning of individual structures, and their properties (geometrical and magnetic), are explored. Localised apolar/polar/ionic bonding, and delocalised bonding is considered. We performed valence bond calculations on the dissociation paths of the polar covalent M–Cl bonds of *tert*-butylchloride ($C(CH_3)_3Cl$, M = C, **1**) and trimethylsilylchloride ($Si(CH_3)_3Cl$, M = Si, **2**). On the reaction pathway, the polarity of these bonds will change. The Si–Cl bond is expected to be more polar than the C–Cl bond. As a reference for these bond dissociation processes, the behaviour during dissociation of a 'pure', apolar, covalent bond, exemplified by H_2, and of an ionic bond, exemplified by NaCl is presented. The curves calculated here could be used in the models of Shaik *et al.*[8]

The delocalised bonding is investigated by a hydrogen model (H_{12}, **3**) that mimics the π-system of benzotricyclobutadiene ($C_{12}H_6$) (analogous to the calculation of pseudo-π currents[9]). Magnetic properties are evaluated for benzene-like structures at a geometry where the inner benzene-moiety has a delocalised π-system (**3b**), and at a geometry where the π-system is localised (**3a**, Chart 2).[10–13]

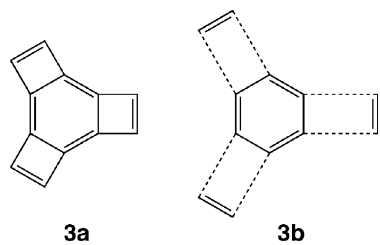

Chart 2 A schematic representation of the geometries used in the VB study on the H_{12} model, which mimics the π-system of benzotricyclobutadiene. At geometry **3a**, the π-system is fully localised, whereas at the geometry **3b**, the π-system is delocalised (benzenoid) [see also Fig. 5].

2. Computational methods

All valence bond calculations were performed with TURTLE,[14] the VB/VBSCF[15,16] module in GAMESS-UK.[17] The basis set used in these calculations was the 6-31G* basis set. The molecules are divided in to two fragments X–Y (to be described below). The wavefunctions, used to obtain the total VB energy, consisted of three structures, *viz*. the covalent (X–Y, **A**, Chart 1), and the two ionic (X^+Y^-, **B** and X^-Y^+, **C**, Chart 1) structures. The energies of the individual structures **A**, **B** and **C** were obtained from three separate calculations in which the wavefunction was built of only one structure (see also Scheme 1). Alternatively, the individual structure energies could be obtained from the VB calculation that includes all structures, however, this approach would suffer even more from the problems described below.

The orbitals of the molecule X–Y were kept strictly localised on the fragments X and Y. Start-up orbitals were generated on the $X^\bullet$ and $Y^\bullet$ fragments separately at the RHF/6-31G* level (Scheme 1b), and were optimised with frozen cores (C: 1s, Si/Na/Cl: 1s, 2s, 2p) at each geometry and for each of the four wavefunctions along the reaction path. With these orbitals, the valence bond wavefunctions for the covalent (**A**), both ionic (**B** and **C**) Lewis structures and the superposition of **A**, **B**, and **C** were constructed (Scheme 1c).

2.1. Reference calculations on H_2 and NaCl

The bond distance of H_2 (X = Y = H) was varied from 0.3 Å to 9.9 Å in steps of 0.1 Å. For NaCl (X = Na, Y = Cl), the curve was calculated from 1.6 Å to 6.0 Å in steps of 0.1 Å, with additional points at 7.0, 8.0, 9.0 and 10.0 Å.

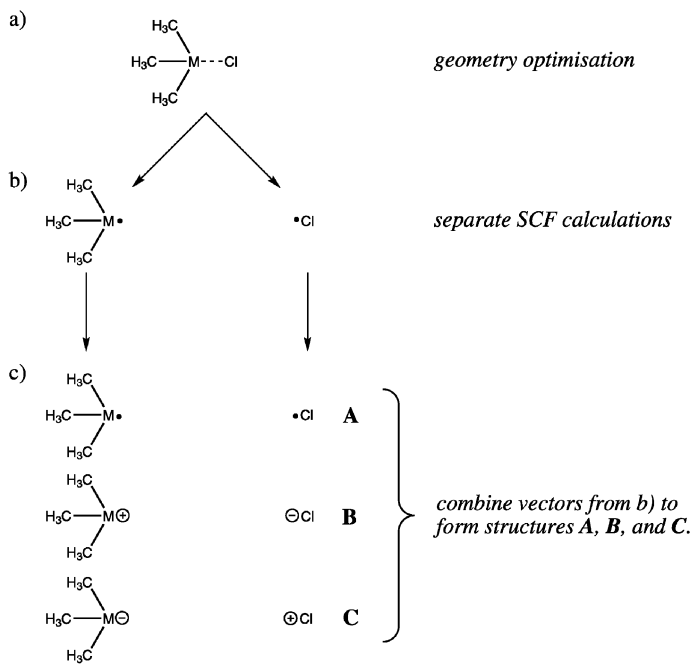

Scheme 1 The three steps to generate the dissociation curves (M = C/Si): (a) Geometry optimisation at fixed M–Cl (dashed) bonds; (b) Generation of start-up orbitals on radical fragments; (c) Valence bond calculations on the three Lewis structures separately (**A**, **B** and **C**) and together (**A** + **B** + **C**).

2.2. Calculations on $C(CH_3)_3Cl$ (1) and $Si(CH_3)_3Cl$ (2)

Twenty-two points on the dissociation paths of $C(CH_3)_3Cl$ (X = $C(CH_3)_3$, Y = Cl, **1**) and $Si(CH_3)_3Cl$ (X = $Si(CH_3)_3$, Y = Cl, **2**) between 1.4 Å and 3.0 Å, with steps of 0.1 Å, with additional points at 3.2, 3.5, 4.0, 5.0 and 10.0 Å have been calculated with fixed lengths for the M–Cl bond (Scheme 1a). The other bond lengths and bond angles were optimised in C_{3v} symmetry at the GVB/6-31G* level,[18] in which the M–Cl σ and M–Cl σ* bonds were correlated. The VB calculations (see Scheme 1) were performed at these geometries.

2.3. Calculations on benzotricyclobutadiene model H_{12} (3)

This model molecule mimics the π-system of benzotricyclobutadiene, and as shown for pyracylene, VB results performed on the hydrogen system are in agreement with π-only VB results.[19] The VB calculations were performed at two geometries, *viz*. one where the hydrogen atoms were placed at the positions of the carbon atoms of the RHF/STO-3G optimised geometry of benzotricyclobutadiene (**3a**), and one where the model cyclobutadieno clamping groups were placed at 2.0 Å from the benzenoid core (**3b**) (Chart 2). The basis set used was the STO-3G basis set, which is sufficient to draw qualitative conclusions about the meaning of resonance structures. At each geometry, two VB calculations were performed to study the benzene-like resonance (Scheme 2), one with a wavefunction consisting of the two benzene resonance structures, and one on just the most important structure (depicted in Chart 2). The cyclobutadieno clamping groups were in all calculations emulated by doubly occupied, localised H–H bonds, taken from an RHF calculation after Pipek Mezey localisation.[20] The magnetisability was calculated at both geometries (**3a** and **3b**), using both VB wavefunctions,[21] and at the RHF level for comparison.

To illustrate the difference in delocalisation, pseudo π-current density plots[9] were calculated using SYSMO,[22] at the CTOCD-DZ[23–25]/STO-3G level of theory. The induced current density is plotted in the molecular plane; diatropic (paratropic) circulation is denoted anticlockwise (clockwise).

3. Results

3.1. Reference calculations on H_2 and NaCl

In Fig. 1 the dissociation curve for H_2 is shown. The total energy curve (E_{tot}), the covalent (E_{cov}) and ionic (E_{ion}) curves are presented.

The total and covalent curves practically coincide over the whole range. This indicates the covalent character of the bond in H_2. For the covalent structure the weight is at least 80% over the whole dissociation range.

In Fig. 2, the dissociation curve for NaCl is shown. At the equilibrium distance (R_0 = 2.4 Å) the Na^+Cl^- structure forms the bonding picture, indicated by its high weight of 0.7. The total energy curve and the ionic curve also almost coincide at this point. Upon dissociation, NaCl splits into $Na^\bullet$ and $Cl^\bullet$, as follows from a weight of 1.0 for the covalent structure, and from the concomitant coincidence of E_{tot} and E_{cov}

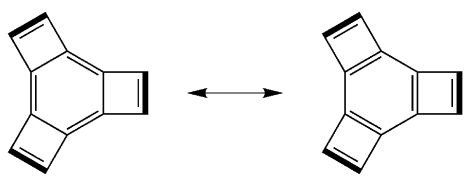

Scheme 2 The benzene-resonance in benzotricyclobutadiene (**3**) is studied with the pseudo-π VB method. The clamping groups, indicated in bold, are described by doubly occupied, localised orbitals.

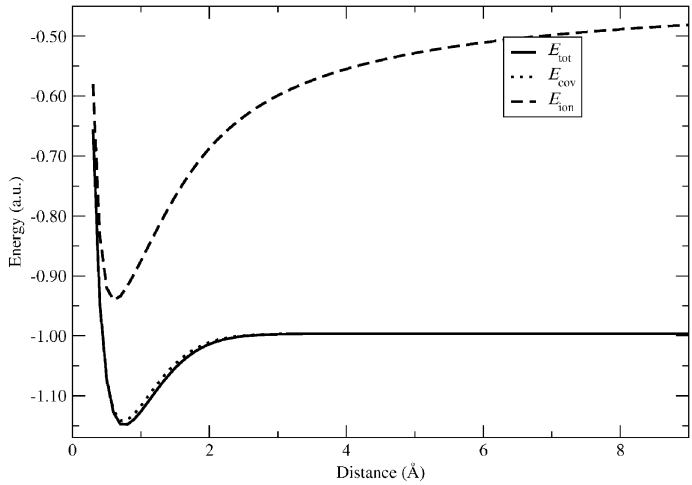

Fig. 1 The dissociation curve of H_2. E_{tot} is the total VB energy, E_{cov} and E_{ion} are, respectively, the energies of the covalent H–H and ionic H^+H^- structures separately.

curves at long distances. The Na^-Cl^+ structure has a negligible contribution (**C**, Chart 1) to the wavefunction over the whole range.

The covalent and ionic curves cross around 5.2 Å. Although the energies for both separate structures are the same, the difference in charge distribution is large: in the covalent case the atoms are neutral, while in the ionic case sodium is positively charged and chlorine negatively charged. In a VB calculation with both structures, the weight of the ionic structure is almost 90% at 5.2 Å. Note that at this crossing the Born–Oppenheimer approximation is not valid any more, but this has no bearing on the following discussion.

The main difference between homolytic bond dissociation of an ionic and covalent bond is the presence (ionic bond)/absence (covalent bond) of a crossing of the ionic

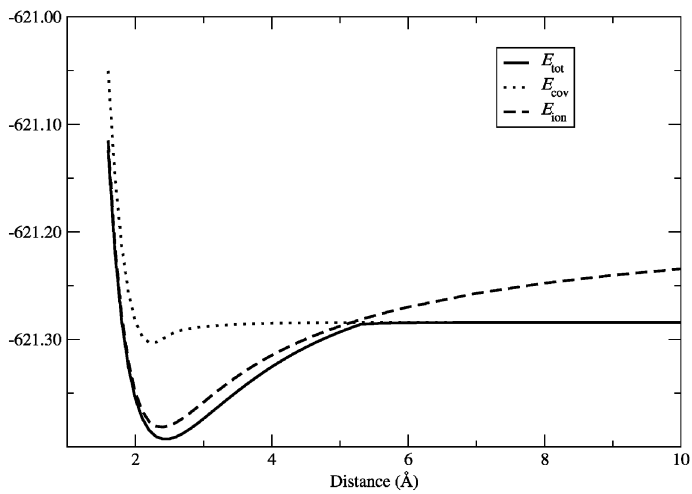

Fig. 2 The dissociation curve of NaCl. E_{tot} is the total VB energy, E_{cov} and E_{ion} are, respectively, the energies of the covalent Na–Cl and ionic Na^+Cl^- structures separately. The curve for Na^-Cl^+ is omitted for clarity, in view of its negligible weight to the total wavefunction.

Table 1 The VB dissociation energy (literature data[26] between parentheses) and optimal M–Cl bond lengths[a]

Compound	E_{dis}/kJ mol^{-1}	R_{M-Cl}/Å
$C(CH_3)_3Cl$ (**1**)	251.4 (234)	1.935
$Si(CH_3)_3Cl$ (**2**)	370.8	2.174

[a] The lowest VB energy and the optimal VB M–Cl bond lengths are obtained by a three-point fit.

and covalent curves. In solution, dissociation to ions can occur,[26,27] and the crossing might be absent.

3.2. Calculations on $C(CH_3)_3Cl$ (1) and $Si(CH_3)_3Cl$ (2)

The optimal M–Cl bond lengths and the corresponding dissociation energies for **1** and **2** are shown in Table 1, and their dissociation curves in Fig. 3 and 4. Both figures contain three curves: the total VB energy (E_{tot}), the energy of the covalent structure **A** (E_{cov}) and the energy of ionic structure **B** (E_{ion}), which corresponds to $M(CH_3)_3{}^+Cl^-$.

The weight for the covalent structure in *tert*-butylchloride (**1**) is at least 66% over the whole range of the curve, thus the C–Cl bond is covalent.

The Si–Cl bond in trimethylsilylchloride (**2**) is more ionic: the weight of the ionic structure is higher than that of the covalent structure between 2.3 Å and 4.1 Å. From 2.0 Å to 4.1 Å, the ionic curve (E_{ion}) lies below the covalent curve (E_{cov}). At 4.1 Å the covalent and ionic curves cross, and the total wavefunction changes vehemently from mainly ionic to covalent character.

An intriguing feature in this figure, not seen in that for **1**, is the barrier in the covalent curve (E_{cov}) at 4.0 Å, near this crossing.

3.3. Calculations on benzotricyclobutadiene model H_{12} (3)

The difference in delocalisation for **3a** and **3b** is evident from the maps of the magnetically induced current density (Fig. 5). For **3a**, localised islands of circulation centred on the formal double bonds are discernible, whereas **3b** sustains a strong

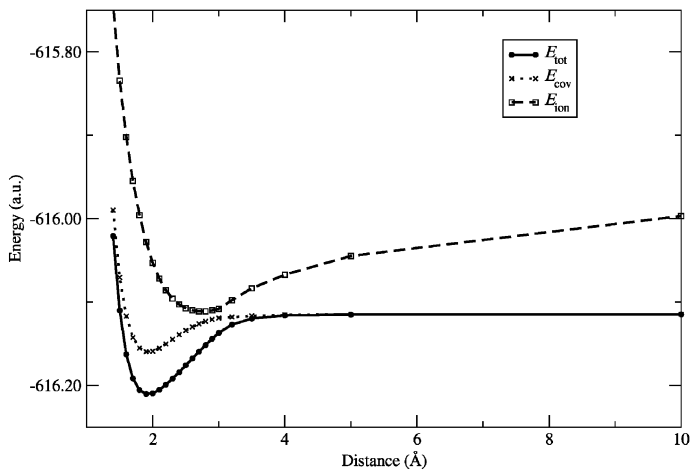

Fig. 3 The dissociation curve of *tert*-butylchloride ($C(CH_3)_3Cl$, **1**). E_{tot} is the total VB energy. E_{cov} is the energy of structure **A** and E_{ion} is the energy of structure **B** separately. The curve for $C(CH_3)_3{}^+Cl^-$ is omitted for clarity.

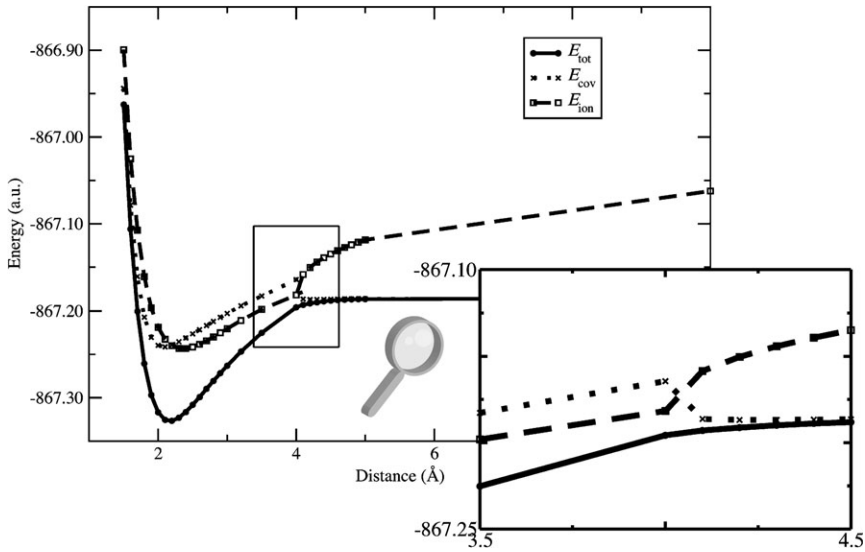

Fig. 4 The dissociation curve of trimethylsilylchloride ($Si(CH_3)_3Cl$, **2**). E_{tot} is the total VB energy. E_{cov} is the energy of structure **A** and E_{ion} is the energy of structure **B** separately. The curve for $Si(CH_3)_3{}^-Cl^+$ is omitted for clarity.

diatropic ring current in the benzene-core, similar to benzene itself.[28] This different magnetic response is reflected in the magnetisabilities of **3a** and **3b**, which are listed in Table 2. The magnetisabilities calculated at geometry **3a** differ markedly from those calculated at geometry **3b**. However, for both **3a** and **3b**, similar magnetisabilities are calculated using the two-structure VB, one-structure VB, and RHF wavefunctions.

4. Discussion

Like the dissociation curves of H_2 and NaCl, those of $C(CH_3)_3Cl$ (**1**) show no irregularities. In contrast, in the covalent dissociation curve of $Si(CH_3)_3Cl$ (**2**) an unexpected discontinuity (barrier) is discernible. This discontinuity can be understood by noting that the reaction pathways for the dissociation of a pure covalent structure and an ionic structure with optimised geometries are different. For a covalent structure, the fragments are both neutral, and the trimethylsilyl radical will

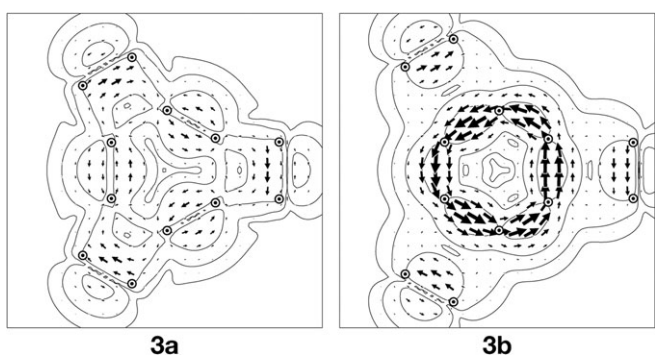

Fig. 5 Pseudo-π maps[9] of the induced current density for **3a** and **3b**, plotted in the molecular plane.

Table 2 The magnetisabilities (au) obtained for the two different **3a** and **3b** H_{12} geometries using the four different VB wavefunctions, and the RHF wavefunction, together with the weights of the two resonance structures in the two-structure wavefunction

	3a		**3b**	
	2 structures	1 structure	2 structures	1 structure
W_1	0.991	1.000	0.886	1.000
W_2	0.023	—	0.114	—
χ_{xx}, χ_{yy}	−29.68	−29.68	−37.54	−37.54
χ_{zz}	−37.09	−37.12	−46.78	−46.77
RHF χ_{xx}, χ_{yy}	−29.62		−37.51	
RHF χ_{zz}	−36.27		−46.71	

remain tetrahedral along the whole curve. For an ionic structure, the trimethylsilyl cation fragment favours the geometry of the cation, in which the silicon and the three carbon atoms are coplanar. In the VB calculations presented here, the wavefunction is the superposition of the covalent and ionic structures, while geometries are optimised in a GVB calculation where *both* structures contribute. The geometry of a covalent/ionic structure obtained by optimisation with the total wavefunction differs from that which would be obtained with only a single structure wavefunction. The use of a single geometry is the underlying assumption of the valence bond resonance picture.

At the crossing, the nature of the total wavefunction changes dramatically from mainly ionic to covalent, and *vice versa*. Concomitant with the change in the wavefunction, the geometry of the fragments changes from nearly coplanar silicon carbon atoms (favoured for ions) to tetrahedral (favoured for radicals). The reaction path that is followed before the crossing is that of the dissociation of the ionic species, and after the crossing it follows the covalent curve. The energy for the covalent structure calculated at the geometries optimised for the total wavefunction (that is mainly the ionic wavefunction) is markedly higher than if the geometry of the fragment was optimised using a wavefunction consisting of only the covalent structure. After the crossing, the geometry changes to that of the covalent structure, leading to a sudden drop in the individual covalent structure energy. The energy of the individual ionic structure increases suddenly, and this is clearly visible as a discontinuity in the curve.

The crossing in the curve of $Si(CH_3)_3Cl$ (**2**) at short distance is not accompanied by any kind of barrier, as the geometry does not change drastically (the structure of the trimethylsilyl fragment cannot change much, due to steric reasons). The ionic and covalent VB structures are *not* orthogonal, and at short distances they have a considerable overlap of 89%.

Discontinuities in individual structure potential energy surfaces, if calculated using a wavefunction that contains multiple structures, are expected to occur when the geometries optimised for each individual structure are significantly different, and the dominant structure-contribution to the total wavefunction changes while moving over the potential energy surface.

The study of delocalised bonds shows another interpretation problem of valence bond structures. The results in Table 2 show that the magnetisabilities are independent of the nature of the wavefunction, and thus independent of the existence of resonance.[21] More interestingly, although the spin-coupling schemes, *i.e.* the Lewis structures, in the one-structure calculation are identical at both geometries **3a** and **3b**, the magnetisabilities differ. This means that the connectivity and overlap between the orbitals determine the response of the wavefunction. These results are in line with the findings for benzene and pyracylene in that the (magnetic) properties of one structure are equal to those obtained when multiple structures are included.[19,21]

Hence, the interpretation of valence bond structures is hampered: there is no direct correspondence between a localised bond, as drawn in a Lewis-structure, and a spin-coupled bond in valence bond theory. The latter is affected by the whole molecule. Concerning aromaticity, this means that the resonance energy, as defined by Pauling, and the ring current criterion are not related.

Conclusions

Decomposition of a wavefunction in structures may be useful for interpretability, but these structures cannot be considered as individual structures. The geometry obtained using a multiple structure wavefunction can differ significantly from that obtained using a single structure wavefunction, leading to inconsistencies on for example potential energy surfaces. The one-to-one correspondence of valence bond structures to Lewis-structures, with localised, independent bonds is absent. The spin-coupled bonds note the presence of the other bonds in the molecule, and therefore identical spin-coupling schemes (valence bond structures) at different geometries, are intrinsically different, furnishing different response properties, independent of resonances.

Acknowledgements

Dr Ir. G. C. Groenenboom (Radboud University, Nijmegen) is gratefully acknowledged for helpful discussions. Partial financial support from The Netherlands Organisation for Scientific Research (NWO, grant 700.53.401 (R. W. A. H.), grant R70-334 (J. J. E.), NWO/NCF, project number SG-032) and European Union (Marie Curie host fellowship, contract number HPMT-CT-2000-00023) is gratefully acknowledged.

References

1 L. Pauling, *J. Am. Chem. Soc*., 1931, **53**, 1367–1400.
2 L. Pauling, *J. Am. Chem. Soc*., 1931, **53**, 3225–3237.
3 L. Pauling, *J. Am. Chem. Soc*., 1932, **54**, 988–1003.
4 L. Pauling, *J. Am. Chem. Soc*., 1932, **54**, 3570–3582.
5 L. Pauling and G. W. Wheland, *J. Chem. Phys*., 1933, **1**, 362–374.
6 L. Pauling, *The Nature of the Chemical Bond and the Structure of Molecules and Crystals: An Introduction to Modern Structural Chemistry*, 3rd edn, Cornell University Press, Ithaca, New York, 1960.
7 B. H. Chirgwin and C. A. Coulson, *Proc. R. Soc. London, Ser. A*, 1950, **201**, 196–209.
8 S. Shaik and A. Shurki, *Angew. Chem., Int. Ed*., 1999, **38**, 586–625, and references therein.
9 P. W. Fowler and E. Steiner, *Chem. Phys. Lett*., 2002, **364**, 259–266.
10 P. W. Fowler, R. W. A. Havenith, L. W. Jenneskens, A. Soncini and E. Steiner, *Chem. Commun*., 2001, 2386–2387.
11 P. W. Fowler, R. W. A. Havenith, L. W. Jenneskens, A. Soncini and E. Steiner, *Angew. Chem., Int. Ed*., 2002, **41**, 1558–1560.
12 R. W. A. Havenith, L. W. Jenneskens and P. W. Fowler, *Chem. Phys. Lett*., 2003, **367**, 468–474.
13 R. W. A. Havenith, L. W. Jenneskens, P. W. Fowler and A. Soncini, *Org. Biomol. Chem*., 2004, **2**, 1281–1286.
14 J. Verbeek, J. H. Langenberg, C. P. Byrman, F. Dijkstra, J. J. Engelberts and J. H. van Lenthe, *TURTLE, An ab initio VB/VBSCF program*, 1988–2005, Utrecht, The Netherlands.
15 J. H. van Lenthe and G. G. Balint-Kurti, *Chem. Phys. Lett*., 1980, **76**, 138–142.
16 J. H. van Lenthe and G. G. Balint-Kurti, *J. Chem. Phys*., 1983, **78**, 5699–5713.
17 M. F. Guest, I. J. Bush, H. J. J. van Dam, P. Sherwood, J. M. H. Thomas, J. H. van Lenthe, R. W. A. Havenith and J. Kendrick, *Mol. Phys*., 2005, **103**, 719–747.
18 W. J. Hunt, P. J. Hay and W. A. Goddard III, *J. Chem. Phys*., 1972, **57**, 738–748.
19 R. W. A. Havenith, *J. Org. Chem*., 2006, **71**, 3559–3563.
20 J. Pipek and P. G. Mezey, *J. Chem. Phys*., 1989, **90**, 4916–4926.
21 R. W. A. Havenith, *Chem. Phys. Lett*., 2005, **414**, 1–5.

22 P. Lazzeretti and R. Zanasi, SYSMO package, University of Modena, 1980. Additional routines by P. W. Fowler, E. Steiner, R. W. A. Havenith, A. Soncini.
23 T. A. Keith and R. F. W. Bader, *Chem. Phys. Lett*., 1993, **210**, 223–231.
24 T. A. Keith and R. F. W. Bader, *J. Chem. Phys*., 1993, **99**, 3669–3682.
25 R. Zanasi, *J. Chem. Phys*., 1996, **105**, 1460–1469.
26 L. Song, W. Wu, Q. Zhang and S. Shaik, *J. Phys. Chem. A*, 2004, **108**, 6017–6024.
27 J. J. Engelberts, J. H. van Lenthe, P. C. Hiberty, L. W. Jenneskens and R. W. A. Havenith, 2006, in preparation.
28 E. Steiner and P. W. Fowler, *Int. J. Quantum Chem*., 1996, **60**, 609–616.

